# Interlayer magnetic coupling: The torque method

V. Drchal and J. Kudrnovský
*Institute of Physics, Academy of Sciences of the Czech Republic, CZ-180 40 Praha 8, Czech Republic*
*and Institute for Technical Electrochemistry, Technical University, A-1060 Vienna, Austria*

I. Turek
*Institute of Physics of Materials, Academy of Sciences of the Czech Republic, CZ-616 62 Brno, Czech Republic*

P. Weinberger
*Institute for Technical Electrochemistry, Technical University, A-1060 Vienna, Austria*
(Received 1 August 1995; revised manuscript received 13 February 1996)

We present *ab initio* calculations of the interlayer exchange coupling between two, in general noncollinearly aligned magnetic slabs embedded in a nonmagnetic spacer. Based on a surface Green's function formalism, two equivalent but formally and physically different approaches are examined and discussed. For the Co/Cu/Co(001) system we demonstrate the usefulness of the concept of infinitesimal rotations in order to calculate the coupling for a finite relative angle $\theta$, in particular for $\theta=\pi$, between the corresponding spin directions in the magnetic slabs. The temperature and layer dependence of the interlayer exchange coupling is examined and the possibility for noncollinear coupling is investigated. [S0163-1829(96)02121-2]

## I. INTRODUCTION

Interlayer oscillatory coupling (IOC) has been found to occur in a number of ferromagnetic-nonmagnetic multilayer systems and is in some cases accompanied by an oscillatory magnetoresistance. A number of models were proposed to explain this phenomenon (for a recent review see Ref. 1). Typically one estimates the energy difference between the ferromagnetic (F) and antiferromagnetic (AF) alignment in order to determine the interaction between two magnetic slabs separated by a nonmagnetic spacer. A slightly different approach was first proposed by Slonczewski.[2] His interaction energy is obtained from the torque by calculating the spin current accross the spacer and employing wave functions. This method was further elaborated by Hathaway and co-workers,[3] Edwards and co-workers,[4] and its usefulness was tested on simple free-electron and tight-binding models. A reformulation of the spin current approach of Slonczewski in terms of Green's functions in a tight-binding representation appeared very recently.[5] Also mentioned has to be an expression for the torque in terms of Green's functions and employing Lloyd's formula for the integrated density of states within a tight-binding model.[6] In Refs. 5 and 6 the change in the grand canonical potential $\delta\Omega(\theta)$ necessary to rotate the spin direction in one slab with respect to another one by an angle $\theta$ is calculated and the torque is expressed as $-\partial\delta\Omega(\theta)/\partial\theta$. Within a nonrelativistic approach this is the most general approach to the problem which in turn also allows for a generalization to random slabs and spacers.

Recently, *ab initio* formulations of the interlayer exchange coupling have appeared,[7–9] based on an application of a layer version of Lloyd's formula in order to evaluate the difference between the grand canonical potentials of the F ($\theta=0$) and AF ($\theta=\pi$) alignment using the so-called frozen potential approximation.[7] In the present paper we generalize our previous approach[8] to the case of an arbitrary angle $\theta$. We also present an alternative formulation of the IOC which, while giving exactly the same result as the original one,[8] differs from it both formally and in its physical interpretation.

The applicability of the method of infinitesimal rotations to various interesting cases, in particular to the AF alignment ($\theta=\pi$), will be studied numerically. Expressions for the bilinear and biquadratic terms in the expansion of the exact formulas are then obtained and their properties, in particular the temperature dependence, studied. All applications are discussed for the Co/Cu/Co(001) system with varying thicknesses of the magnetic slabs and of the spacer.

## II. FORMALISM

The grand canonical potential $\Omega$ of a system is defined by

$$\Omega=-\frac{1}{\pi}\mathrm{Im}\int_{-\infty}^{\infty} f(E)\mathrm{Tr}\ \ln\mathscr{G}(z)dE, \tag{1}$$

where $z=E+i0$, $f(E)$ is the Fermi-Dirac distribution function, and Tr denotes the trace over the spin and configuration space. Within the tight-binding linear muffin-tin orbital[10] (TB-LMTO) method $\mathscr{G}(z)$ is given by

$$\mathscr{G}(z)=[P(z)-S]^{-1}, \tag{2}$$

where $S$ is a matrix of structure constants $S_{\mathbf{R},\mathbf{R}'}$, $P(z)$ is a site-diagonal matrix of potential functions $P_{\mathbf{R}}(z)$ which in spin space can be written as the following $2\times2$ supermatrices:

 

$$P_{\mathbf{R}}(z)=\begin{pmatrix} P_{\mathbf{R}}^{\uparrow\uparrow}(z), & P_{\mathbf{R}}^{\uparrow\downarrow}(z) \\ P_{\mathbf{R}}^{\downarrow\uparrow}(z), & P_{\mathbf{R}}^{\downarrow\downarrow}(z) \end{pmatrix},$$

$$S_{\mathbf{R},\mathbf{R}'}=\begin{pmatrix} S_{\mathbf{R},\mathbf{R}'}^{\uparrow\uparrow} & 0 \\ 0 & S_{\mathbf{R},\mathbf{R}'}^{\downarrow\downarrow} \end{pmatrix},$$

$$S_{\mathbf{R},\mathbf{R}'}^{\uparrow\uparrow}=S_{\mathbf{R},\mathbf{R}'}^{\downarrow\downarrow}, \tag{3}$$

and $\mathbf{R}$ and $\mathbf{R}'$ denote site indices. The off-diagonal terms of $P_{\mathbf{R}}(z)$ in spin space account for a spin orientation of atoms in one and the same magnetic layer with respect to a (fictious) global axis of the system. The use of the so-called auxiliary Green's function (GF) defined in (2) in Eq. (1) instead of the physical Green's function is justified within the TB-LMTO formalism (see e.g., Ref. 11). It should be noted that in the absence of spin-orbit coupling only the relative angle between the spin orientations in two different magnetic layers is important.

The system considered consists of a central finite nonmagnetic spacer slab ($\mathscr{C}$) of varying thickness $N$ and two semi-infinite systems, denoted $\mathscr{L}$ (left) and $\mathscr{R}$ (right), each containing $M$ magnetic layers on top of a semi-infinite nonmagnetic spacer. In the limit this model represents two semi-infinite magnetic slabs sandwiching the nonmagnetic spacer. The reference frame of a rotation of the spin orientation in one particular slab by an angle $\theta$ is assumed to be with respect to the ferromagnetic alignment ($\theta=0$). In particular, we assume that the spin orientation in the right magnetic slab $\mathscr{R}$ is rotated by an angle $\theta$ with respect to that of the left magnetic slab $\mathscr{L}$.

The quantity of the physical interest is the difference of the grand canonical potentials between the ferromagnetic ($\theta=0$) and a rotated ($\theta\neq 0$) alignment of the two magnetic slabs, namely the exchange energy $\mathscr{E}_x(\theta)=\Omega(\theta)-\Omega(0)$. The exchange energies $\mathscr{E}_x(\theta)$ are very small quantities and their direct evaluation is rather cumbersome.[1] The clue is to use Lloyd's formula in the framework of the frozen potential approximation as applied to a rotated alignment which differs from the ferromagnetic alignment by a localized perturbation.[6–8] Technically there are few possibilities how to divide the system into an unperturbed part and a localized perturbation. A common approach[6,7] is to consider the ''rotated'' magnetic slab as a perturbation. Clearly, with increasing thickness $M$ of the magnetic slabs the numerical effort increases as the third power of $M$. This limitation can be relaxed[8] by considering three decoupled noninteracting regions $\mathscr{L}$, $\mathscr{C}$, and $\mathscr{R}$ as an unperturbed system. The localized perturbation is the interlayer coupling at the $\mathscr{L}/\mathscr{C}$ and the $\mathscr{C}/\mathscr{R}$ interfaces, which is independent of the thickness of the magnetic slabs. The concept of principal layers[12] (PL) as used within the TB-LMTO method leads to a block tridiagonal form of the structure constants and of the inverse of the GF. Employing the partitioning technique with respect to the trace of the logarithm of the GF,[8] it is possible to extract directly the term describing the coupling of interfaces, $\delta\mathrm{Tr}\ \ln\mathscr{G}(z)$,

$$\delta\mathrm{Tr}\ \ln\mathscr{G}(z)=-\frac{1}{N_\parallel}\sum_{\mathbf{k}_\parallel}\ \mathrm{tr}\ \ln[1-\tau_1(\mathbf{k}_\parallel,z)g_{1N}(\mathbf{k}_\parallel,z)\times\tau_N(\mathbf{k}_\parallel,z)g_{N1}(\mathbf{k}_\parallel,z)], \tag{4}$$

where the $t$ matrices $\tau_i$ $(i=1,N)$

$$\tau_i(\mathbf{k}_\parallel,z)=\Gamma_i(\mathbf{k}_\parallel,z)[1-g_{ii}(\mathbf{k}_\parallel,z)\Gamma_i(\mathbf{k}_\parallel,z)]^{-1} \tag{5}$$

are defined in terms of the effective embedding potentials $\Gamma_i(\mathbf{k}_\parallel,z)$ at the $\mathscr{L}/\mathscr{C}$ $(i=1)$ and the $\mathscr{C}/\mathscr{R}$ $(i=N)$ interfaces,

$$\Gamma_1(\mathbf{k}_\parallel,z)=S_{10}(\mathbf{k}_\parallel)\widetilde{\mathscr{G}}(\mathbf{k}_\parallel,z)S_{01}(\mathbf{k}_\parallel), \tag{6}$$

$$\Gamma_N(\mathbf{k}_\parallel,z)=S_{01}(\mathbf{k}_\parallel)\mathscr{G}(\mathbf{k}_\parallel,z)S_{10}(\mathbf{k}_\parallel).$$

A standard $\mathbf{k}_\parallel$ Fourier transform was performed in (4). In Eqs. (4) and (5), $g_{11}(z)$,$g_{1N}(z)$,$g_{N1}(z)$, and $g_{NN}(z)$ are the corresponding blocks of the spacer slab GF consisting of $N$ layers, tr denotes the trace over angular momenta ($L=\ell m$) and spin ($\sigma=\uparrow,\downarrow$), and $S_{01}(\mathbf{k}_\parallel)$ and $S_{10}(\mathbf{k}_\parallel)$ are the interlayer structure constants which couple neighboring PL's. Finally, in (6) $\widetilde{\mathscr{G}}(\mathbf{k}_\parallel,z)$ and $\mathscr{G}(\mathbf{k}_\parallel,z)$ are the surface Green's functions[12,13] (SGF's) of the magnetic subsystems $\mathscr{L}$ and $\mathscr{R}$, respectively. The coupling between the two magnetic subsystems is due to the layer off-diagonal projections $g_{1N}(\mathbf{k}_\parallel,z)$ and $g_{N1}(\mathbf{k}_\parallel,z)$ of the GF of the finite slab spacer. The oscillatory behavior of the interlayer coupling is then governed by the oscillatory behavior of these quasi-one-dimensional spacer Green's functions, a formulation which is very much in the spirit of a simplified RKKY approach.[1]

Alternatively, one can consider as the unperturbed system two semi-infinite systems, $\mathscr{L}'$ and $\mathscr{R}'$, coupled together via interlayer coupling at a single interface $\mathscr{L}'/\mathscr{R}'$. The $\mathscr{L}'$ subsystem consists of $M$ magnetic layers on top of a semi-infinite nonmagnetic spacer similarly as in the previous case, i.e., $\mathscr{L}'\equiv\mathscr{L}$. The $\mathscr{R}'$ subsystem contains, in addition, the finite spacer slab on top of the magnetic slab, namely it consists of the previous $\mathscr{C}$ and $\mathscr{R}$ subsystems, i.e., $\mathscr{R}'=\mathscr{C}\cup\mathscr{R}$. In other words, we shall consider the difference between the rotated and ferromagnetic alignments indirectly in terms of the energy of a single interface rather than directly as the interface-interface interaction energy as in the previous case. Employing again the partitioning technique to the trace of the logarithm one gets

$$\delta\mathrm{Tr}\ \ln\mathscr{G}(z)=-\frac{1}{N_\parallel}\sum_{\mathbf{k}_\parallel}\ \mathrm{tr}\ \ln[1-\Gamma_{\mathscr{L}'}(\mathbf{k}_\parallel,z)\mathscr{G}_{\mathscr{R}'}(\mathbf{k}_\parallel,z)], \tag{7}$$

$$\Gamma_{\mathscr{L}'}(\mathbf{k}_\parallel,z)=S_{10}(\mathbf{k}_\parallel)\mathscr{G}_{\mathscr{L}'}(\mathbf{k}_\parallel,z)S_{01}(\mathbf{k}_\parallel),$$

where, similar to (6), the quantity $\Gamma_{\mathscr{L}'}(\mathbf{k}_\parallel,z)$ has the meaning of an effective embedding potential, and $\mathscr{G}_{\mathscr{L}'}$ and $\mathscr{G}_{\mathscr{R}'}$ are the corresponding SGFs. Both expressions, Eqs. (4) and (7), give exactly the same result for $\mathscr{E}_x$. It should be noted that an addition of spacer layers introduces changes only in $\mathscr{G}_{\mathscr{R}'}$ but leaves $\mathscr{G}_{\mathscr{L}'}$ unchanged. Since $\mathscr{G}_{\mathscr{R}'}$ is related to the local density of states[12,13] of the top surface layer of the $\mathscr{R}'$ subsystem, the formulation in (7) resembles rather a quantum-well state description (see, e.g., Ref. 1) of the IOC than the RKKY-like approach of Eq. (4). Equation (7) is also more convenient from a numerical point of view as the determination of the SGF (Ref. 12) is more efficient than the evaluation of the layer off-diagonal blocks $g_{1N}(z)$ and $g_{N1}(z)$ of the Green's function of the spacer slab $\mathscr{C}$. In par-

ticular the formulation in (7) is similar in spirit to the spin-current approach of Ref. 5 formulated within a semiempirical tight-binding model.

Let us now turn to our primary problem, namely the evaluation of the energy difference between arbitrary alignments. Consider the following quantity:

$$\mathrm{tr}\ \ln Z = \mathrm{tr}\ \ln(1-A_0B) - \mathrm{tr}\ \ln(1-A_0B_0), \tag{8}$$

where the matrices $A_0$ and $B_0$ are related to the ferromagnetic alignment and thus are diagonal in spin space

$$A_0=\begin{pmatrix} A_0^{\uparrow} & 0 \\ 0 & A_0^{\downarrow} \end{pmatrix}, \quad B_0=\begin{pmatrix} B_0^{\uparrow} & 0 \\ 0 & B_0^{\downarrow} \end{pmatrix}. \tag{9}$$

The particular form of the subblocks $A_0^{\sigma}$ and $B_0^{\sigma}$ ($\sigma=\uparrow,\downarrow$) is given by

$$A_0^{\sigma} = g_{N1}(\mathbf{k}_{\parallel},z)\,\tau_1^{\sigma}(\mathbf{k}_{\parallel},z)\,g_{1N}(\mathbf{k}_{\parallel},z),$$

$$B_0^{\sigma} = \tau_N^{\sigma}(\mathbf{k}_{\parallel},z), \tag{10}$$

and

$$A_0^{\sigma} = S_{10}(\mathbf{k}_{\parallel})\,\mathscr{G}^{\sigma}_{\mathscr{L}'}(\mathbf{k}_{\parallel},z)\,S_{01}(\mathbf{k}_{\parallel}),$$

$$B_0^{\sigma} = \mathscr{G}^{\sigma}_{\mathscr{R}'}(\mathbf{k}_{\parallel},z), \tag{11}$$

for the formulations based on Eq. (4) and Eq. (7), respectively.

The matrix $B$ refers to an alignment in which the orientations of the spin in two magnetic slabs are rotated relatively by an angle $\theta$,

$$B = U(\theta)B_0U^{\dagger}(\theta), \tag{12}$$

where

$$U(\theta)=\begin{pmatrix} c & s \\ -s & c \end{pmatrix} \tag{13}$$

is the rotation matrix[14] for spin 1/2, $c=\cos(\theta/2)$, $s=\sin(\theta/2)$, $U(\theta)U^{\dagger}(\theta) = U^{\dagger}(\theta)U(\theta)=1$, and $\det U(\theta) = \det U^{\dagger}(\theta)$. The quantity $1-A_0B$ in (8) can therefore be written as

$$1-A_0B = (U(\theta)-A_0U(\theta)B_0)U^{\dagger}(\theta), \tag{14}$$

where, as follows from Eqs. (9) and (13),

$$U(\theta)-A_0U(\theta)B_0=\begin{pmatrix} c(1-A_0^{\uparrow}B_0^{\uparrow}) & s(1-A_0^{\uparrow}B_0^{\downarrow}) \\ -s(1-A_0^{\downarrow}B_0^{\uparrow}) & c(1-A_0^{\downarrow}B_0^{\downarrow}) \end{pmatrix}. \tag{15}$$

Using now the identity $\mathrm{tr}\ \ln X = \ln\ \det X$, which is valid for any non-singular matrix $X$, and the identity

$$\det\begin{pmatrix} A & B \\ C & D \end{pmatrix} = \det A\cdot\det D\cdot\det(1-A^{-1}BD^{-1}C), \tag{16}$$

which in turn is valid if the matrices $A$ and $D$ are nonsingular, it is straightforward to prove that

$$\mathrm{tr}\ \ln Z = \mathrm{tr}_L \ln\left(1-\frac{1-\cos(\theta)}{2}M\right), \tag{17}$$

where

$$M = 1-(1-A_0^{\uparrow}B_0^{\uparrow})^{-1}(1-A_0^{\uparrow}B_0^{\downarrow}) \times (1-A_0^{\downarrow}B_0^{\downarrow})^{-1}(1-A_0^{\downarrow}B_0^{\uparrow}). \tag{18}$$

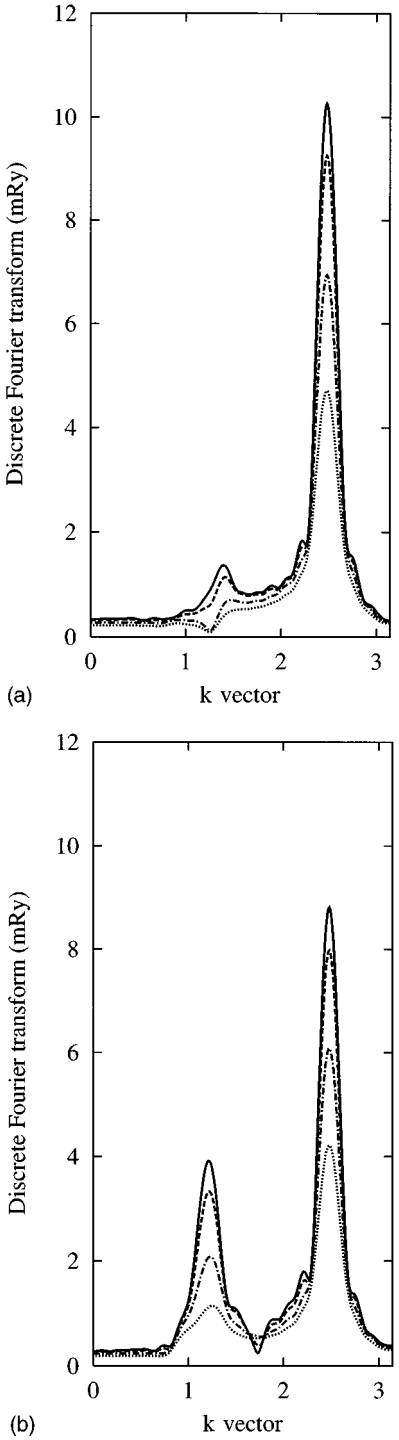


FIG. 1. Absolute value of the discrete Fourier transform of $N^2\mathscr{E}_x(\pi,N)$ for a finite set of spacer layers ($N=10$–$50$) and for different temperatures: (a) two semi-infinite Co(001) subsystems sandwiching the Cu spacer, and (b) two 5 monolayer thick Co(001) slabs in fcc Cu. The temperatures are $T=0$ K (full line), $T=150$ K (dashed line), $T=300$ K (dash-dotted line), and $T=450$ K (dotted line).

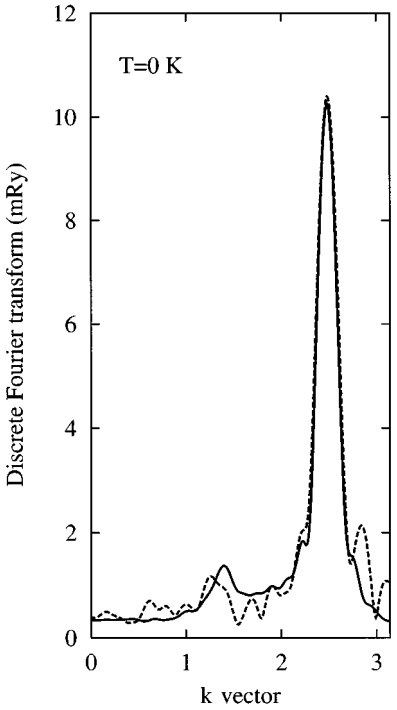


FIG. 2. Absolute value of the discrete Fourier transform of $N^2\mathscr{E}_x(\pi,N)$ for a finite set of spacer layers ($N=10$–$50$, full line and $N=40$–$80$, dashed line) corresponding to two semi-infinite Co(001) subsystems sandwiching the Cu spacer. The temperature is $T=0$ K in both cases.

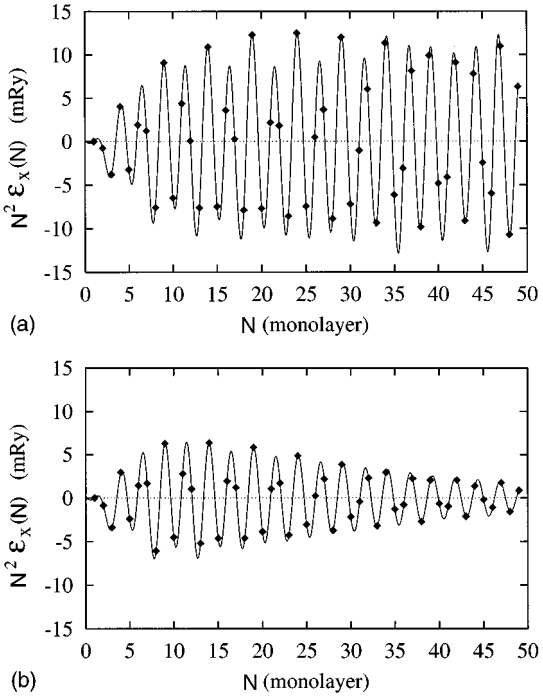


FIG. 3. Exchange coupling $N^2\mathscr{E}_x(\theta,N)$ as a function of the spacer thickness $N$ for two semi-infinite Co(001) subsystems sandwiching the Cu spacer: (a) $T=0$ K, and (b) $T=450$ K. Diamonds refer to the calculated values, the full line (back Fourier transform) serves as a guide to the eye.

It should be noted that in (8) tr denotes the trace over orbital momenta and spin, while in (17) $\mathrm{tr}_L$ denotes the trace over orbital momenta only. The final expression for $\mathscr{E}_x(\theta)$ is thus given by

$$\mathscr{E}_x(\theta)=\frac{1}{\pi N_\parallel}\sum_{\mathbf{k}_\parallel}\ \mathrm{Im}\int_C f(z)\times \mathrm{tr}_L \ln\left(1-\frac{1-\cos(\theta)}{2}M(\mathbf{k}_\parallel,z)\right)dz, \qquad (19)$$

in which the energy integral is formulated in terms of a contour integral which will be discussed in detail in Sec. III A. For the antiferromagnetic alignment, i.e., for $\theta=\pi$, it is straightforward to verify the equivalence of Eqs. (10), (18), and (19) with those given in our previous paper.[8] It is also possible to show that Eqs. (11), (18), and (19) are formally related to the results of the spin-current approach[5] as formulated within a Green's function formalism based on an empirical single orbital tight-binding model. Finally, it should be mentioned that in the related approach[6] which employs as unperturbed part the infinite spacer with two magnetic slabs of the thickness $M$, the numerical effort increases as $M^3$ contrary to the present approach, which scales linearly with $M$.

Since the rotations in the spin space, Eq. (13), form a Lie group, the torque formula can be easily obtained by differentiating Eq. (19) with respect to the angle $\theta$. By definition one gets therefore

$$T(\theta)=-\frac{\partial\mathscr{E}_x(\theta)}{\partial\theta}\ \text{ or }\ \mathscr{E}_x(\theta)=-\int_0^\theta T(\theta')d\theta', \qquad (20)$$

whereby $T(\theta)$ follows immediately from (19),

$$T(\theta)=\frac{\sin(\theta)}{2\pi N_\parallel}\sum_{\mathbf{k}_\parallel}\ \mathrm{Im}\int_C f(z)\mathrm{tr}_L \times\left[M(\mathbf{k}_\parallel,z)\left(1-\frac{1}{2}[1-\cos(\theta)]M(\mathbf{k}_\parallel,z)\right)^{-1}\right]dz. \qquad (21)$$

Finally, by formally expanding the logarithm in (19) in powers of $1-\cos(\theta)$, one can cast the expression for $\mathscr{E}_x(\theta)$ into the form

$$\mathscr{E}_x(\theta)=A_1[1-\cos(\theta)]+\frac{1}{2}B_1[1-\cos(\theta)]^2+\cdots, \qquad (22)$$

where $A_1$ and $B_1$ are the bilinear and the biquadratic exchange coupling coefficients, respectively,

$$A_1=\frac{1}{2\pi N_\parallel}\sum_{\mathbf{k}_\parallel}\ \mathrm{Im}\int_C f(z)\mathrm{tr}_L M(\mathbf{k}_\parallel,z)dz, \qquad (23)$$

$$B_1=-\frac{1}{4\pi N_\parallel}\sum_{\mathbf{k}_\parallel}\ \mathrm{Im}\int_C f(z)\mathrm{tr}_L[M(\mathbf{k}_\parallel,z)]^2dz.$$

It should be noted that in the literature[6] other forms of $\mathscr{E}_x(\theta)$ are also used, e.g.,

$$\mathscr{E}_x(\theta)=E_0-A_2\cos(\theta)-B_2\cos^2(\theta)+\cdots. \qquad (24)$$

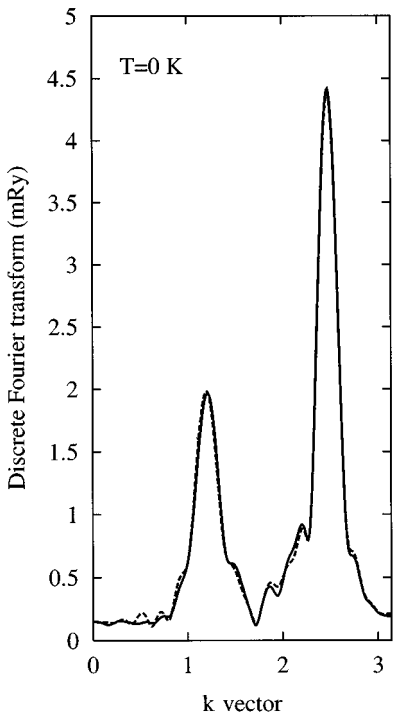


FIG. 4. Absolute value of the discrete Fourier transform of the torque $N^2T(\theta,N)$ (full line) and of $N^2\mathscr{E}_x(\theta,N)$ (dashed line) for a finite set of spacer layers ($N=10$–$50$) and for $\theta=\pi/2$. This case refers to two 5 ML thick Co(001) slabs and $T=0$ K.

While the interrelation of the above two forms [(23) and (24)] is trivial, certain care is needed when comparing different theoretical results or experimental data as the $A$'s and the $B$'s differ both by value and even sign.

From (19) follows the possibility for an expansion around the state with a given angle $\theta$ different from zero. Of particular interest of course is the expansion of $\mathscr{E}_x(\theta)$ for a small $\theta$, i.e., when $1-\cos(\theta)$ is a small parameter [the method of infinitesimal rotations (MIR's)]. This approach becomes particularly relevant in the case when the spacer is a magnetic metal or for complicated geometries, e.g., for periodic multilayers. The applicability of the MIR to magnetic spacers is based on the validity of the local force theorem for magnetic systems, the usefulness of which was demonstrated for the case of bulk magnetic crystals and their alloys.[15]

## III. NUMERICAL RESULTS AND DISCUSSION

### A. Details of calculations

The numerical studies were performed for Co(001) slabs in a fcc-Cu spacer assuming an ideal lattice corresponding to the experimental lattice spacing of fcc Cu. Self-consistent potentials of bulk Cu and of a single Co(001) monolayer in bulk Cu are used also for the interacting slabs (the frozen potential approximation[7,8,16]). Special care was devoted to the energy and the Brillouin zone integrations: at a finite temperature[7–9] an integration along a contour $C$, which encloses the first few Matsubara frequencies and which starts and ends at $E_{\min}$ and $E_{\max}$, respectively, is performed using a Gaussian quadrature procedure. The energy $E_{\min}$ refers to the valence band bottom while $E_{\max}$ lies sufficiently above the Fermi energy $E_f$ in order to include also the partially filled states (for details see Ref. 17). For $T=0$ K we have tested two contours, namely a semicircle between $E_{\min}$ and $E_f$, or, alternatively, a line contour $E_f+i\varepsilon$, $\varepsilon\in(0,\infty)$, and

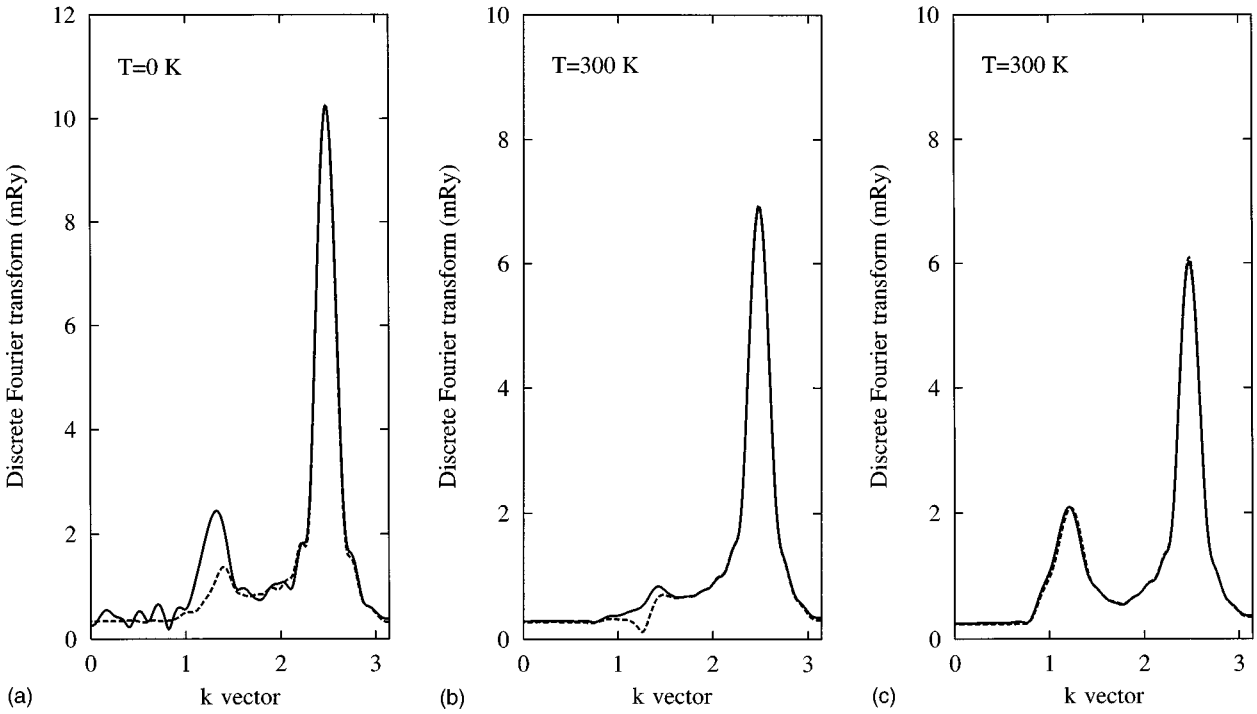


FIG. 5. Absolute value of the discrete Fourier transform of $N^2\mathscr{E}_x(\pi,N)$ (dashed line) and of $N^2A_1(N)[1-\cos(\theta)]$ (solid line) for a finite set of spacer layers ($N=10$–$50$) and for $\theta=\pi$: (a) two semi-infinite Co(001) subsystems sandwiching the Cu spacer, $T=0$ K, (b) the same but for $T=300$ K, (c) two 5 monolayer thick Co(001) slabs, $T=300$ K.

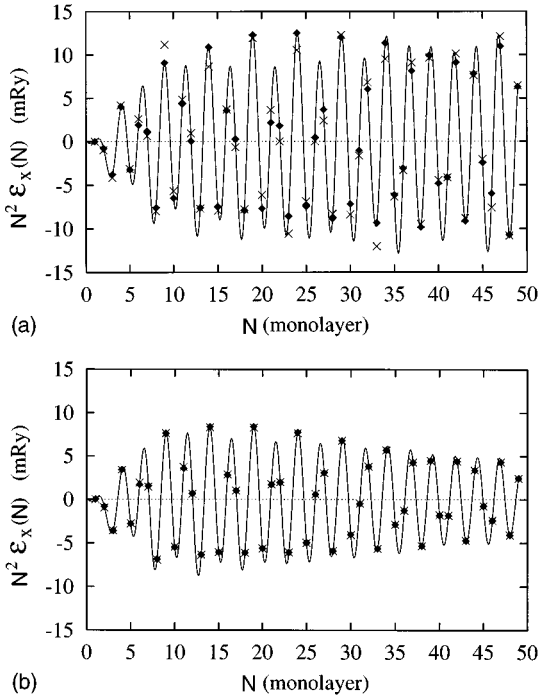


FIG. 6. Exchange coupling $N^2\mathscr{E}_x(\theta,N)$ (diamonds) and the bilinear term $N^2A_1(N)[1-\cos(\theta)]$ (crosses) for $\theta=\pi$ as a function of the spacer thickness $N$ for two semi-infinite Co(001) subsystems sandwiching the Cu spacer; (a) $T=0$ K, and (b) $T=300$ K. The full line (back Fourier transform) serves as a guide to the eye.

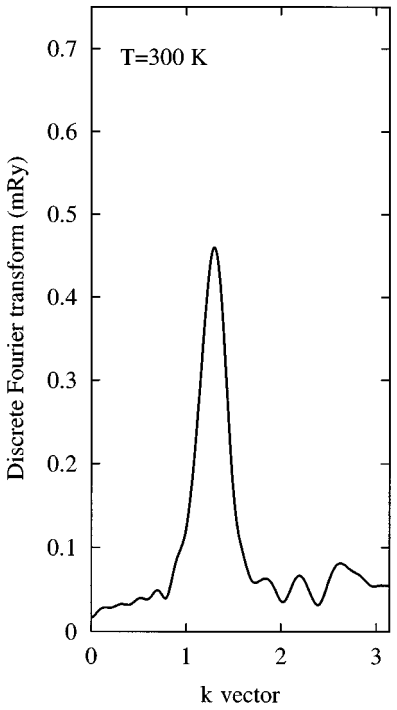


FIG. 7. Absolute value of the discrete Fourier transform of the biquadratic term $N^2B_1(N)$ for a finite set of spacer layers ($N=10$–$50$) corresponding to two semi-infinite Co(001) subsystems sandwiching the Cu spacer. The temperature is $T=300$ K.

again using a Gaussian quadrature. The results were very similar in both cases. The use of the line contour allows one to avoid possible problems connected with the phase of a complex logarithm. Typically a total of 20–25 energy points was used. A large number of $\mathbf{k}_\parallel$ points in the irreducible 2D Brillouin zone is needed only for the energy points close to the real axis, whereby generally a greater number is needed for lower temperatures and thicker spacers. The number of $\mathbf{k}_\parallel$ points can be significantly reduced for energies well off the real axis. For higher temperatures the first Matsubara frequencies move deeper into the complex plane, making again the $\mathbf{k}_\parallel$ integrations numerically less demanding.[7] In particular, for the first four energy points we used 4095/2485/1035/325 $\mathbf{k}_\parallel$ points in the irreducible 2D Brillouin zone and 55 for all remaining energy points on the contour. The thickness of the spacer was in most cases varied from 1 to 50 layers and in particular cases from 1 to 80 layers. Finally, the self-consistent potential of a monolayer Co(001) slab in bulk fcc-Cu was also employed for a slab 5 monolayers thick and for a semi-infinite Co(001) system. We have verified that essentially the same results are obtained using potentials of pure fcc-Cu and fcc-Co crystals aligned to a common Fermi energy of the spacer.

### B. Analysis of the results

The calculated results, namely $\mathscr{E}_x(\theta,N)$, where $N$ specifies the spacer thickness, were analyzed in two ways. First, a discrete Fourier transform

$$F(k)=\frac{1}{p}\sum_{N=N_{\min}}^{N_{\max}} N^2\mathscr{E}_x(\theta,N)\exp(ikN),$$

where $p=N_{\max}-N_{\min}$ is the number of values used in the Fourier analysis, and $N_{\min}$ is chosen in order to eliminate the effect of very thin spacers (typically $N_{\min}=10$ and $N_{\max}=50$). The periods of oscillations $\Lambda_i$ (in monolayers) are then identified with the positions $k_i$ of pronounced peaks of the absolute value $|F(k_i)|$ of a discrete Fourier transform $F(k)$ as $\Lambda_i=2\pi/k_i$, while the amplitudes of oscillations $A_i$ are estimated from $A_i=(2/p)|F(k_i)|$. The background oscillations thus obtained (see Figs. 1, 2, 4, 5, 7 below) are due to the finite data sets used for the Fourier transformation. The background oscillations could be smoothened using the procedure described in Ref. 18, namely by multiplying $N^2\mathscr{E}_x(\theta,N)$ by $C\sin(\pi N/p)/(\pi N/p)$, where $C$ is a normalization factor. Second, the values for $N^2\mathscr{E}_x(\theta,N)$ are displayed as a function of the spacer thickness $N$. Both representations are consistent with a RKKY-like behavior of $\mathscr{E}_x(\theta,N)$, namely $\mathscr{E}_x(\theta,N)\propto N^{-2}$ for a large $N$.

### C. The expansion of the exact expression, Eq. (19)

The aim of this subsection is to study the validity of the expansion of the logarithm in Eq. (19) in powers of $[1-\cos(\theta)]/2$ or, alternatively, in powers of $\cos(\theta)$, for a general angle $\theta$ and thus to justify limited expansions, Eqs. (23) and (24). The logarithm in (19) can be expanded into the Taylor series

$$\mathscr{E}_x(\theta)=-\sum_n \frac{1}{n}\lambda^n m_n, \quad \lambda=\frac{1-\cos\theta}{2}, \tag{25}$$

$$m_n=\frac{1}{\pi N_\parallel}\sum_{\mathbf{k}_\parallel}\mathrm{Im}\int_C f(z)\,\mathrm{tr}_{\mathbf{L}}(M(\mathbf{k}_\parallel,z))^n dz, \tag{26}$$

in terms of the moments $m_n$. The expansion is absolutely convergent for $|\lambda|<1/M$, where $M$ is the maximum absolute value of the eigenvalues of the matrix $M(\mathbf{k}_\parallel,z)$ for all $\mathbf{k}_\parallel$ vectors from the surface Brillouin zone, and for all energies $z$ on the contour $C$ used in (26). Note that the matrix $M$ depends on the energy $z$, $\mathbf{k}_\parallel$ vector, the spacer thickness $N$, and on the orbital indices $\ell m$ in a very complicated manner. Clearly, the expansion is convergent for the infinitesimally small $\theta$, but its extension to finite $\theta$'s is not straightforward. In order to investigate numerically its convergence we calculated the first 60 moments for thick Co slabs at $T=0$ K and at $T=300$ K numerically and found that for low temperatures and small spacer thicknesses, the series is divergent, while for larger spacer thicknesses and higher temperatures it becomes convergent. The convergence is rather fast for spacer thicknesses $N\geqslant 30-35$ layers at $T=0$ K, and for $N\geqslant 8-10$ layers at $T=300$ K. The same behavior was found also for Co slabs 5 monolayers thick.

It is worthwhile to mention that even if the series in (25) diverges, its first few terms are very close to the exact result. This can be seen from Fig. 5 where we compare $N^2\mathscr{E}_x(\theta,N)$ and $2N^2A_1(N)$ as a function of the spacer thickness $N$. For $T=0$ K the difference between the exact expression and the bilinear (Heisenberg-like) approximation becomes smaller with increasing $N$ and is negligible for all spacer thicknesses for $T=300$ K.

This kind of behavior is typical for an asympotic expansion. It can be explained in the following way. The $n$th moment $m_n$ can be viewed as sum of the $n$th powers of the eigenvalues of the matrix $M$ evaluated for a set of arguments $\{\mathbf{k}_\parallel,z\}$ with proper weights. We have calculated the eigenvalues of the matrix $M$ and have found that most of them lie inside the unit circle of the complex plane. Only a small fraction (not exceeding 1% in the most unfavorable case) falls outside the unit circle.

### D. Results for Co/Cu/Co(001) system

A discrete Fourier transform of the temperature dependence of $\mathscr{E}_x(\theta,N)$ for the collinear arrangement $\theta=\pi$ is plotted in Fig. 1 for the cases of 5 monolayer (ML) slabs and semi-inifinite Co(001) slabs. For $T=0$ K the results coincide with those of Ref. 16 but with the background oscillations smoothed by using the procedure described above. We find a nearly complete suppression of the long period oscillations for thick Co(001) slabs (see also[8,9,16]). For finite slabs, however, both the short and the long period oscillations exist,[7–9, 16] in particular for 5 ML thick Co(001) slabs. The periods of oscillations are in a fair agreement with existing experiments[19] as well as with other theoretical approaches.[7,9,19] It was demonstrated recently[16] that the amplitudes of oscillations for real samples, in particular the short period oscillations, may be strongly reduced due to the presence of disorder in the system (interfacial roughness and interfacial interdiffusion between magnetic and nonmagnetic subsystems). In addition, a suppression of the amplitudes of oscillations due to the temperature is found, which is nonnegligible for room and higher temperatures. It turns out that the effect of temperature is somewhat stronger for the long periods (the case of 5 ML's slabs) than for the short periods.

The results are insensitive to the choice of the subset of $N^2\mathscr{E}_x(\pi,N)$ values used for a discrete Fourier transform as illustrated for the case of thick Co(001) slabs in Fig. 2. As compared to the subset $N=10-40$ greater background oscillations for the subset $N=40-80$ layers indicate a slight decrease of relative accuracy of calculations for very thick spacers. Similar results were obtained also for Co slabs 5 ML's thick.

For semi-ininfinite Co slabs the temperature dependence of $\mathscr{E}_x(\pi,N)$ as a function of spacer thickness $N$ is presented in Fig. 3 for $T=0$ K and $T=450$ K. The results are in accordance with predictions of a simple RKKY model,[19] namely that the suppression of oscillations is proportional to the temperature $T$ and the spacer thickness $N$ via a certain function of the factor $\zeta=NT$. As can be seen from Fig. 1, finite temperatures result in overall smaller values of the amplitudes, while a suppression of exchange coupling with increasing spacer thickness $N$ is clearly seen in Fig. 3 (case $T=450$ K). It should be noted that due to the dependence on the $\zeta$ factor the amplitudes of oscillations now depend on the particular subset of $N^2\mathscr{E}_x(\pi,N)$ values used for the discrete Fourier analysis. A comparison of discrete Fourier transforms has to be confined, therefore, to the same subset.

In order to illustrate numerically the relation between the torque $T(\theta,N)$, Eq. (21), and the exchange coupling $\mathscr{E}_x(\theta,N)$, Eq. (19), in Fig. 4 we present for Co slabs 5 ML thick results for a discrete Fourier transform of both quantities at $\theta=\pi/2$, $T=0$ K. For symmetry reasons, the torque $T(\theta)$ is zero for collinear alignments of the magnetic slabs, i.e., for $\theta=0$ or $\theta=\pi$, and has a maximum for $\theta=\pi/2$. The very good quantitative agreement between $T(\pi/2)$ and $\mathscr{E}_x(\pi/2)$ as obtained also for thick Co slabs is quite remarkable. Even better agreement is obtained at higher temperatures. It is easy to verify from Eqs. (19) and (21) that for the leading term of the expansion one gets

$$\mathscr{E}_x(\theta,N)\cong A_1(N)[1-\cos(\theta)]$$

and

$$T(\theta,N)\cong A_1(N)[1-\cos(\theta)]\sin(\theta),$$

i.e., $T(\pi/2)=-\mathscr{E}_x(\pi/2)$. The above discussion on the convergence of the Taylor expansion for $\mathscr{E}_x(\theta)$ with respect to $[1-\cos(\theta)]$ applies therefore also to a similar expansion for $T(\theta)$.

### E. Bilinear and biquadratic couplings

In the following we want to illustrate the range of validity of the approximate expansion in Eq. (19), and, in particular, its approximation by the bilinear and biquadratic terms, Eqs. (23) and (24). Bilinear coupling [the first terms in (23) and (24)] is exact for infinitesimally small $\theta$ but we deliberately tested its applicability in the extreme limit of $\theta=\pi$. Then $\mathscr{E}_x(\pi,N)\approx 2A_1(N)$ and the corresponding results are displayed in Figs. 5 and 6. Irrespective of the thickness of the magnetic slabs the present calculations confirm a good overall agreement between $\mathscr{E}_x(\pi,N)$ and its approximate form $2A_1(N)$ already for $T=0$ K and almost perfect agreement for $T=300$ K. Quite obviously, the Heisenberg-like or bilinear terms in the exact expression (19) yield already a very

accurate description of the coupling, in particular for $T \geqslant 300$ K, while the non-Heisenberg terms, in particular the biquadratic terms, are negligible for higher temperatures and large spacer thicknesses. In other words, temperature has a more pronounced effect on the biquadratic terms than on the bilinear terms. Seemingly, the angle dependence of $\mathscr{E}_x(\theta,N)$ is then correctly approximated by $\mathscr{E}_x(\theta,N) \approx A_1(N)[1-\cos(\theta)]$. The present calculations confirm therefore that this approximation can be used not only for small angles $\theta$ but for any $\theta \leqslant \pi$. As discussed in Sec. II, it seems that by starting from the ferromagnetic alignment and by using subsequently the MIR, accurate estimates for $\mathscr{E}_x(\theta,N)$ for the case of more complicated geometries like periodic multilayers with in general more complex spin structures can be obtained.

A discrete Fourier transform of the biquadratic term $N^2B_1(N)$, Eq. (23), as well as its dependence as a function of the spacer thickness is shown in Figs. 7 and 8, respectively, for the case of thick Co slabs and for $T=300$ K. The existence of the long period oscillations for the biquadratic term is a consequence of the so-called aliasing.[19] The frequency is doubled in the biquadratic term as compared to the bilinear one, i.e., the value of the corresponding $k$ vector in the discrete Fourier transform of the biquadratic term is $k_b = 2 \times 2.48 = 4.96$. The corresponding irreducible vector[19] is $k_b = |2 \times \pi - \mathrm{k}_b| = 1.32$ which is in excellent agreement with the value $k_b = 1.31$ in Fig. 7. The absolute value of the biquadratic term, however, is much smaller as compared to the bilinear term. Temperature suppresses the oscillations of the biquadratic term similarly as for $\mathscr{E}_x(\theta,N)$ [compare Fig. 3(b)].

### F. Remark on the $\pi/2$ coupling

Finally we want to address the question of an energetically favored orthogonal arrangement of the spin orientations in two semi-infinite Co(001) subsystems sandwiching the Cu spacer. By definition, the inequalities $\mathscr{E}_x(\pi/2,N) < \mathscr{E}_x(0,N)$ and $\mathscr{E}_x(\pi/2,N) < \mathscr{E}_x(\pi,N)$ should be fulfilled for a certain spacer thickness $N$ at the same time. For this study we used the exact expression (19) because of the convergence problems for the Taylor series expansion for low temperatures and thin spacers. We have considered different geometrical models, namely the case of an ideal interface (the intrinsic $\pi/2$ coupling) and the case of the interface roughness. The motivation for such study comes from recent studies by Slonczewski[20,21] in which he suggested that either the interface roughness[20] or so-called loose spins[21] could be responsible for the $\pi/2$ coupling. In order to discuss the case of interfacial roughness, we assume as in the previous paper[16] large flat terraces of monolayer heights fluctuating randomly and uncorrelated in both directions around an ideal interface with the probability $r$, followed by a simple statistical average with respect to the average spacer thickness $N$.

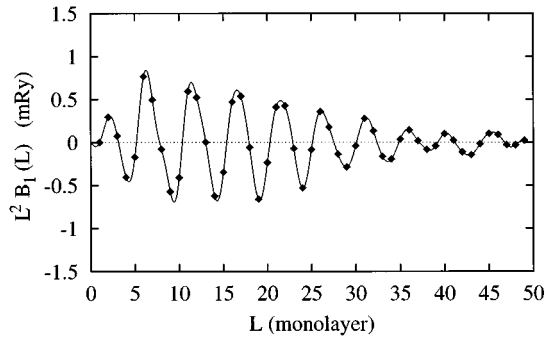


FIG. 8. The biquadratic coupling $N^2B_1(N)$ as a function of the spacer thickness $N$ for two semi-infinite Co(001) subsystems sandwiching the Cu spacer. The temperature is $T=300$ K. Diamonds refer to the calculated values, the full line (back Fourier transform) serves as a guide to the eye.

We have found no $\pi/2$ coupling for the case of an ideal interface. On the other hand, the $\pi/2$ coupling is energetically favorable for the probabilities $r=0.2$ and $r=0.25$, but no such coupling was found for $r=0.05$ and $r=0.1$. Consistent with these results, a $\pi/2$ coupling occurs more frequently for $r=0.25$. The same calculations performed for $T=300$ K still give a $\pi/2$ coupling for $r=0.2$ and $r=0.25$ but for a smaller number of layers. This in turn is consistent with the dominating bilinear coupling for higher temperatures as discussed above.

## IV. CONCLUSIONS

We have derived a closed expression for the exchange coupling between two magnetic subsystems separated by a nonmagnetic spacer with a relative angle $\theta$ between the corresponding spin orientations. The derivation is based on a surface Green's function formalism and the numerical effort needed to evaluate the resulting expression scales linearly with the thickness of both the spacer and the magnetic slabs. A particular case of our expression is the torque formula for a general angle $\theta$.

A detailed analysis of the temperature dependence of exchange coupling was performed for the trilayer Co/Cu/Co(001) in the frozen potential approximation. In particular, a strong temperature dependence of the non-Heisenberg-like terms as compared with the Heisenberg-like ones was found.

The Taylor expansion of the exchange coupling with respect to the small parameter $1-\cos(\theta)$ was found to converge sufficiently well only for thick spacers, and to be strongly temperature dependent. The bilinear or the Heisenberg-like term seems to dominate the expansion for temperatures equal or higher than the room temperature.

We also demonstrated the usefulness of the method of infinitesimal rotations with respect to a ferromagnetic alignment of magnetic slabs since it can serve as an interpolation scheme for arbitrary angles of $\theta$. This result in particular indicates the possibility of an approximate evaluation of the exchange coupling for more complex geometries than the trilayer arrangement studied here and also studied in most of the other theoretical treatments.

Finally, we have verified that interface roughness favors a noncollinear coupling, specifically a $\pi/2$ coupling, as compared with the case of an ideal interface (the intrinsic $\pi/2$ coupling). A more detailed study of this phenomenon is necessary in the future by considering other layer stackings than the fcc(001) and other spacer and magnetic slab materials or geometrical arrangements.

## ACKNOWLEDGMENTS

Financial support for this work was provided by the Grant Agency of the Czech Republic (Project Nos. 202/93/1174 and 202/93/0688), the Center for the Computational Materials Science (GZ 45.384), and the Austrian Science Foundation (P10231).

[1] K.B. Hathaway, *Ulrathin Magnetic Structures II*, edited by B. Heinrich and J.A.C. Bland (Springer, Berlin, 1994), p. 45.
[2] J.C. Slonczewski, Phys. Rev. B **39**, 6995 (1989).
[3] K.B. Hathaway and J.R. Cullen, J. Magn. Magn. Mater. **104-107**, 1840 (1992); R.P. Ericksson, K.B. Hathaway, and J.R. Cullen, Phys. Rev. B **47**, 2626 (1993).
[4] D.M. Edwards, J.M. Ward, and J. Mathon, J. Magn. Magn. Mater. **126**, 380 (1993).
[5] D.M. Edwards, A.M. Robinson, and J. Mathon, J. Magn. Magn. Mater. **140-144**, 517 (1995).
[6] J. d'Albuquerque e Castro, M.S. Ferreira, and R.B. Muniz, Phys. Rev. B **49**, 16 062 (1994).
[7] P. Lang, L. Nordström, R. Zeller, and P.H. Dederichs, Phys. Rev. Lett. **71**, 1927 (1993).
[8] J. Kudrnovský, V. Drchal, I. Turek, and P. Weinberger, Phys. Rev. B **50**, 16 105 (1994).
[9] L. Nordström, P. Lang, R. Zeller, and P. Dederichs, Phys. Rev. B **50**, 13 058 (1994).
[10] O.K. Andersen and O. Jepsen, Phys. Rev. Lett. **53**, 2571 (1984).
[11] J. Kudrnovský and V. Drchal, Phys. Rev. B **44**, 7515 (1990); V. Drchal, J. Kudrnovský, L. Udvardi, and P. Weinberger, *ibid.* **45**, 14 328 (1992).
[12] B. Wenzien, J. Kudrnovský, V. Drchal, and M. Šob, J. Phys.: Condens. Matter **1**, 9893 (1989).
[13] J. Kudrnovský, I. Turek, V. Drchal, P. Weinberger, N.E. Christensen, and S.K. Bose, Phys. Rev. B **46**, 4222 (1992).
[14] See, for example, A. Messiah, *Quantum Mechanics* (North-Holland, Amsterdam, 1969), Vol. II, Appendix C.
[15] A.I. Liechtenstein, M.I. Katsnelson, V.P. Antropov, and V.A. Gubanov, J. Magn. Magn. Mater. **67**, 65 (1987).
[16] J. Kudrnovský, V. Drchal, I. Turek, M. Šob, and P. Weinberger, Phys. Rev. B **53**, 5125 (1996).
[17] K. Wildberger, P. Lang, R. Zeller, and P.H. Dederichs, Phys. Rev. B **52**, 11 502 (1995).
[18] C. Lanczos, *Applied Analysis* (Dover, New York, 1988), p. 219.
[19] P. Bruno and C. Chappert, Phys. Rev. B **46**, 261 (1992).
[20] J.C. Slonczewski, Phys. Rev. Lett. **67**, 3172 (1991).
[21] J.C. Slonczewski, J. Appl. Phys. **73**, 5957 (1993).